

The University of Manitoba

Myelin Development in Young Hydrocephalic Rats

by

Yi Wei Zhang

**Submitted to the Faculty of Graduate Studies in partial fulfillment of the
requirements for the degree of Master of Science**

**Department of Pathology
Faculty of Medicine, Winnipeg, Manitoba
August, 1997**

0-612-23570-X

The author retains ownership of the copyright in this thesis. Neither the thesis nor substantial extracts from it may be printed or otherwise reproduced without the author's permission.

L'auteur conserve la propriété du droit d'auteur qui protège cette thèse. Ni la thèse ni des extraits substantiels de celle-ci ne doivent être imprimés ou autrement reproduits sans son autorisation.

The author has granted a non-exclusive licence allowing the National Library of Canada to reproduce, loan, distribute or sell copies of this thesis in microform, paper or electronic formats.

L'auteur a accordé une licence non exclusive permettant à la Bibliothèque nationale du Canada de reproduire, prêter, distribuer ou vendre des copies de cette thèse sous la forme de microfiche/film, de reproduction sur papier ou sur format électronique.

Our file / Notre référence

Your file / Votre référence

Bibliothèque nationale
du Canada
Acquisitions et
services bibliographiques
395, rue Wellington
Ottawa ON K1A 0N4
Canada

National Library
of Canada
Acquisitions and
Bibliographic Services
395 Wellington Street
Ottawa ON K1A 0N4
Canada



**THE UNIVERSITY OF MANITOBA
FACULTY OF GRADUATE STUDIES

COPYRIGHT PERMISSION PAGE**

MYELIN DEVELOPMENT IN YOUNG HYDROCEPHALIC RATS

BY

YI WEI ZHANG

**A Thesis/Practicum submitted to the Faculty of Graduate Studies of The University
of Manitoba in partial fulfillment of the requirements of the degree
of
MASTER OF SCIENCE**

Yi Wei Zhang 1997 (c)

**Permission has been granted to the Library of The University of Manitoba to lend or sell
copies of this thesis/practicum, to the National Library of Canada to microfilm this thesis
and to lend or sell copies of the film, and to Dissertations Abstracts International to publish
an abstract of this thesis/practicum.**

**The author reserves other publication rights, and neither this thesis/practicum nor
extensive extracts from it may be printed or otherwise reproduced without the author's
written permission.**

Abstract

Hydrocephalus is a neurological disorder characterized by excessive cerebrospinal fluid (CSF) accumulation in enlarged ventricular cavities inside the brain. Hydrocephalus is associated with gradual progressive impairment and destruction of cerebral white matter. To investigate the potential for reversibility of these changes, hydrocephalus was induced in three week old rats by injection of kaolin into cisterna magna. Ventricle size was confirmed by MR imaging. Ultrastructural changes within the corpus callosum, the number of axons per unit area, and myelin thickness were assessed. Myelin proteolipid protein (PLP) and axon growth associated protein (GAP-43) were assayed in cerebrum by Northern blot and immunoblot. GAP-43 protein also was measured by immunohistochemistry. Axon transport function was detected by retrograde labeling of Fluoro-Gold tracer.

At one week hydrocephalus, the myelin sheath around axons greater than $0.4\mu\text{m}$ diameter was abnormally thin, PLP protein was significantly reduced, axons per unit area were less, and GAP-43 protein was increased in the periventricular white matter. PLP and GAP-43 mRNAs were up-regulated. Axonal transport appeared to be normal in two week hydrocephalic rats. With persistent hydrocephalus at four weeks, axons were destroyed, and PLP protein decreased, however myelin sheath developed an appropriate thickness around existing axons, and GAP-43 protein remained elevated.

Shunt treatment of hydrocephalus at one week prevented severe damage to axons and myelin. The PLP and GAP-43 mRNAs and proteins were maintained at intermediate levels between hydrocephalus and controls.

These data suggest that early hydrocephalus delays myelination in young rat brains. Up-regulated mRNA of PLP suggests an attempt to increase synthesis of myelin protein and recover retarded myelination. GAP-43 changes suggest that neurons rapidly respond to hydrocephalic injury and adjust their functional state to prepare for stress. In immature hydrocephalic rat brain, there is a potential to develop normal myelin sheaths if axons survive.

Table of Contents

Title Page

Certificate of Examination

Table of Contents

Acknowledgments

Abstract

List of Figures

List of Tables

1.0	Review of the Literature	page 1
1.1	Introduction	
1.2	The Pathological Changes of hydrocephalus	
1.3	Animal Models of Experimental hydrocephalus	
1.4	Treatment by Shunting	
1.5	The Myelin Structure and Production	
1.6	Models of Demyelination and Altered myelination	
1.7	Elements of Involved in Myelin and Axon Regeneration	
1.8	Axon Regeneration	
1.9	Summary	
1.10	Hypotheses	
2.0	Materials and Methods	page 15
2.1	Induction of Hydrocephalus	
2.2	Magnetic Resonance Imaging	
2.3	Diversional Shunting of CSF	
2.4	Transmission Electron Microscopy	
2.5	Northern Hybridization Analysis	
2.6	In Situ hybridization	
2.7	Western Immunoblotting	
2.8	Immunohistochemistry	
2.9	Fluoro-Gold Tracer Pressure Injection	
2.10	Data Analysis	

3.0	Results	page 23
3.1	Ventricular Enlargement	
3.2	Ultrastructure of Corpus Callosum	
3.3	PLP mRNA and Protein	
3.4	GAP-43 mRNA and Protein	
3.5	Retrograde Neuronal Labeling	
4.0	Discussion	page 32
5.0	References	page 37

Acknowledgments

I wish to express my sincere thanks to Dr. Marc Del Bigio, my supervisor, for his valuable teaching, supervision, encouragement and guidance. Many thanks to Drs. Nance and Bruni who acted on my advisory committee and provided suggestions for the project and thesis.

I thank the Department of Pathology which provided me with the opportunity to complete my graduate studies. My appreciation is expressed to Dr. Adamson and everyone in the Department for their help. Financial assistance for the project was provided by the Manitoba Health Research Council.

I thank Cathy Crook for her excellent technical assistance, and Dr. Richard Buist for producing the MR images.

Dr. Delange deserves thanks for my first year training in Human Genetics, and Drs. Geitz and Bhullar for their advice.

Words cannot express my gratitude to my mother and family members for their constant support and encouragement.

List of Figures

1. **Magnetic resonance images** page 23a
2. **Transmission electron micrographs of myelin** page 24a
3. **Transmission electron micrographs of damaged axon** page 25a
4. **PLP in situ hybridization** page 27a
5. **PLP mRNA Northern blots** page 27a
6. **PLP protein Western blot** page 27a
7. **GAP-43 in situ hybridization** page 28a
8. **GAP-43 mRNA Northern blots** page 28a
9. **GAP-43 protein Western blot** page 29a
10. **GAP-43 immunohistochemistry** page 29a

List of Tables

1.	Ventricle size	page 23
2.	Corpus callosum thickness	page 24
3.	Axon quantities	page 25
4.	Myelin thickness	page 26
5.	PLP mRNA levels	page 27
6.	PLP protein levels	page 28
7.	GAP-43 mRNA levels	page 29
8.	GAP-43 protein levels	page 29
9.	GAP-43 immunohistochemistry	page 30
10.	FluoroGold retrograde transport	page 30

1.0 Review of the Literature

1.1 Introduction

Hydrocephalus is a neurological disorder characterized by excessive cerebrospinal fluid (CSF) accumulation in enlarged ventricular cavities inside the brain. The dilation of the cerebral ventricles can damage surrounding brain tissues, cause a functional brain deficit, and if uncontrolled may cause brain stem herniation and death.

Normally, the choroid epithelial cells within the ventricular system produce 80% of CSF. The CSF flows along a pressure gradient from the lateral to the third ventricle then to the fourth ventricle. The CSF enters the subarachnoid space surrounding the central nervous system (CNS) via the foramina of the fourth ventricle, then passes through the arachnoid villi and enters the venous sinuses. Lymphatic channels that exist adjacent to the sites of nerve root exit are also important for CSF absorption⁶⁸.

Hydrocephalus can be classified into two types: (1) Non-obstructive, in which there is an excessive formation of CSF, for example choroid plexus tumors. This is very rare. (2) Obstructive, in which obstruction to CSF flow occurs anywhere along its pathway⁹³.

1.2 The Pathological Changes of Hydrocephalus

(1) Ventricles

Ventricular enlargement in the absence of primary brain atrophy is the principle feature of hydrocephalus. The most affected region is the lateral ventricle. Ventriculomegaly is the result of blocked normal flow of CSF or decreased CSF absorption ²⁴.

(2) White Matter

Periventricular white matter shows obvious edema with marked expansion of extracellular space and increased water content. The white matter can have a spongy appearance or even gross cavitation ^{27, 41, 47, 48, 100}. The edema might be caused by abnormal permeability of blood vessels in white matter, a flow of CSF into brain by higher intraventricular pressure ^{37, 71}, or an abnormal transependymal absorption ⁸⁶. Thinning of the cerebrum reflects primarily the loss of white matter which is associated with a significant loss of lipid, protein, myelin and axons ^{24, 41, 92, 106}.

Axons in periventricular white matter are stretched and lost ^{27, 41, 52, 71, 75, 92, 112}. It was suggested that the demyelination is probably due to white matter edema, pressure ischemia and consequent anoxia ^{24, 27}. Delayed myelination has been reported in young hydrocephalic animals and infants with ventriculomegaly ^{9, 27, 61}.

Cerebrovascular changes have also been implicated in white matter damage. The elevated CSF pressure and physical distortion of the brain altered the architecture of blood vessels. Fewer capillaries and narrowed caliber of capillaries

may lead to reduction of cerebral blood flow and caused brain ischemia ^{24, 25, 27, 37}.

The susceptibility of white matter to hypoxic/ischemic damage in immature brain probably is the result of increased energy demands during myelinogenesis ^{11, 27}.

(3) Gray Matter

Gray matter may also be affected. There is evidence that the complexity of the neuronal dendritic trees is reduced ⁴³, the cortical synaptic density is decreased ⁵⁷, and synaptogenesis appears to be impaired in congenital hydrocephalic rats ^{76, 77}. Adult humans with severe hydrocephalus show a higher prevalence of cortical neurons with neurofibrillary tangles and there may be pancortical gliosis and neuronal loss ²⁸. However, minimal changes have been reported in the basal ganglia ²⁴.

(4) Ependyma and Subependyma

Ependymal cells possess the chemical and mechanical machinery to act as a barrier against the passage of potentially neurotoxic substance from the CSF into the brain ²². Ependymal stretching, flattening, disruption, as well as macrophage attachment to ependyma are common features in hydrocephalus ^{10, 24, 85, 86, 112}. Cilia and microvilli are progressively lost ^{25, 106}, and the ependyma is focally denuded or totally destroyed with only clusters of cells persisting. The damage is dependent on the severity of ventriculomegaly ²⁴. Although ependymal cells are highly susceptible to injury and have little regenerative capacity ^{14, 93, 112}, nevertheless, Del

Bigio and Bruni (1988) ²⁵ demonstrated increased ependymal cell proliferation following hydrocephalic induction in adult rabbits.

Subependymal cells have substantial regenerative powers ⁹³. They are able to proliferate and differentiate into astroglia, oligodendroglia or neurons under certain condition ⁶⁹. Certain stimuli, such as pressure changes and stretching, may mobilize subependymal germinal cells to participate in replacement of ependymal cells ²⁴. In hydrocephalus, there is a significant increase in the number of subependymal stem cells surrounding the ventricle, and they exhibit significantly increased mitotic activity ^{10, 26, 112}.

1.3 Animal Models of Experimental Hydrocephalus

Dandy and Blackfan (1913) ²⁰ produced the first experimental hydrocephalus model by plugging the cerebral aqueduct of dogs with cotton. Afterwards, different experimental animals were used including kittens, cats, puppies, dogs, mice, rats, rabbits and monkeys. Methods or materials used to induce hydrocephalus include bacteria, viruses, blood, lampblack, India ink, gelatin, balloons, silicone oil and kaolin ^{21, 47, 49}. Many of these methods involved extensive surgical procedures and some methods failed to produce predictable results ²¹. Kaolin and silicone oil induced hydrocephalus are the most commonly used models at present. But it is more difficult to control the anatomical location of the obstruction with silicone than with kaolin ⁵¹. Injection of kaolin into the cisterna magna produces a mild

inflammatory reaction which encircles the brain stem, blocks the subarachnoid space, and causes hydrocephalus ²¹. Hirayama (1980) ⁴⁷ compared nine animal models of hydrocephalus and concluded that the age of the animals and the methods for inducing hydrocephalus are the primary factors determining the final pathological findings ²⁴.

1.4 Treatment by Shunting

Shunting is presently the most widely used treatment for hydrocephalus in humans. CSF shunting diverts CSF from the lateral ventricle to another body space by means of a silicone elastomer tube and valve system. It is believed that shunting can provide relief to brain by lowering intracranial pressure reducing the size of ventricles, reducing the flow of CSF into periventricular tissue, and restoring cerebrum thickness and blood flow ^{24, 48, 92}. Some investigators considered that the reconstitution of the cerebrum by shunting did not result in reformation of lost elements, but rather in preservation of the remaining elements ^{92, 101, 114}. However, shunting must be performed early, in order for the pathological changes to be reversible. Early shunting decreases periventricular edema, increase the number of patent capillaries, improves blood flow and appears to permit the regeneration and/or repair of the myelin sheath ²⁴. Following shunting the plasma/CSF amino acid ratio and the glucose metabolism in white matter returns to normal ^{23, 27, 89}. Shunting also partially restores the number of synapses and overall size of neurons

67, and largely prevented neuronal structure abnormalities 9, 44. If shunting is performed late, it fails to prevent damage. Both ependyma and periventricular capillaries may fail to re-establish their normal configuration and damaged axons persist, and limited remyelination occurs 19, 24, 27, 48.

1.5 The Structure and Production of Myelin

The myelin sheath allows saltatory conduction of nervous impulses at a greater velocity, frequency, and efficiency. It shields axons from local toxic factors, such as pathogenic cytokines, and ionic disturbances 46, 73. Various minor myelin proteins, including enzymes are involved in lipid synthesis and metabolism, protein degradation, phosphorylation-dephosphorylation, ion transport, and signal transduction 46.

The major myelin proteins are thought to be largely structural. Proteolipid protein (PLP) and myelin basic protein (MBP) together make up 60-80% of total myelin proteins. They are mainly responsible for the ordered lamellar arrangement of the myelin sheath. The PLP functions in compaction of intraperiod line of myelin. Its mRNA transcripts are most abundant in oligodendrocytes that are assembling myelin sheath. PLP gene produces two mRNAs, PLP and DM-20, by alternate splicing of its transcript product. DM-20, the smaller isoform of PLP, contains all sequences except the latter part of exon 3 6. DM-20 mRNA is detected in the neural tube in development and persists throughout embryonic life 105, while

PLP is expressed postnatally during the final stages of maturation of oligodendrocytes ¹⁰⁴. Thus, DM-20 protein appears prior to extensive accumulation of PLP in rat and human brain ^{38, 59, 60}. Thus, DM-20 protein may function as a non-myelin protein in differentiating oligodendrocytes at very early stage ^{6, 105}. MBP has at least six isoforms and has an important role in either development or maintenance of the myelin sheath, and compaction of the major dense line of myelin ^{46, 53}. Minor structural proteins are also present, and include myelin associated glycoprotein (MAG), myelin-oligodendrocyte associated protein (MOG), and other glycoproteins.

1.6 Models of Demyelination and Altered Myelination

It is known that many factors can cause loss of myelin. Demyelination may be primary or may occur secondary to axonal damage ⁶⁴. The animal models of CNS demyelination are useful to identify the molecular, cellular and morphological events and factors in myelin repair or remyelination ^{32, 72, 73}. In principle, there are three categories of animal models of demyelination and remyelination.

(1) Immune mediated: Demyelination can be mediated through autoantibodies; antibody-mediated complement activation, macrophage attack on myelin sheath by phagocytosis ; release of inflammatory mediators, such as oxygen free radicals, proteases, and cytokines which cause dissociation of myelin or T lymphocyte derived TNF-alpha and lymphotoxin. These factors may play a role in

diseases such as multiple sclerosis and experimental autoimmune encephalomyelitis 32, 72, 73.

(2) **Virus mediated:** Numerous viruses can induce demyelination in animals. There are two mechanisms to explain their pathogenicity; either direct infection of oligodendrocytes or immune mediated response secondary to viral infection.

Thieler's virus infection is a well characterized model 64, 72.

(3) **Toxin mediated:** Toxins can produce localized lesions due to direct toxic effect on oligodendrocytes or the myelin sheath. Once a toxin is withdrawn, rapid spontaneous remyelination occurs. The myelin repair may be rapid and complete.

Cuprizone and trimethyltin are examples of this 64, 72

Myelin production may also be delayed at the time of brain development.

(1) **Delay caused by malnutrition:** The degree of delayed myelination depends on the severity of malnutrition, the duration of malnutrition, and the brain developmental period affected. The delay of myelination is characterized by significantly reduced percentage of myelinated axon fibers, disproportionately reduced width of the myelin sheath, and an altered relationship between the axon diameter and myelin sheath thickness. This suggests that the initiation and/or progression of myelination is retarded and these effects are likely due to a reduction in the number of oligodendrocytes generated from the subependymal zone 58.

(2) **Metabolic disease and neonatal diseases:** Many metabolic diseases can cause a delay in myelination, possibly due to toxic effects of abnormal metabolites 56. In human neonatal diseases, delayed myelination is considered to be the consequences of impaired oligodendroglia, or disturbances to rapidly growing axons 61.

(3) Drugs and chemicals: Myelin, because of its long half-life, is especially vulnerable to lipid peroxidation and other chemical reactions, and can accumulate lipophilic substances. Anticonvulsants, ethanol and other agents applied to developing brain generally retards synthesis of myelin either by depressing the rate of myelin membrane synthesis or causing abnormal glial maturation ¹¹³.

Finally, numerous mutations affecting myelination have been identified in rodents and other animals including humans. They have provided great insight into the molecular mechanisms of formation and maintenance of myelin. The Shiverer mouse, which has a large portion of the MBP gene deleted, exhibits a total absence of MBP. These mice lack the major dense line in myelin and are severely hypomyelinated ⁹⁰. The Jimpy mouse has a point mutation in the PLP gene. Related other components of myelin in the CNS are also reduced, probably owing to oligodendrocyte death ^{66, 96}. Although Quaking mice have normal PLP and MBP genes, they show an apparent delay in expressing these two genes ^{66, 96, 97}. In Mld mice, the MBP gene is duplicated in tandem, and is associated with hypomyelination of the CNS ¹⁸.

1.7 Elements Involved in Myelin and Axon Regeneration

Many experiments suggested that the subependymal zone is the most important site of regenerating new oligodendrocytes ^{15, 32, 53, 63, 84}. However, not all

experiments supported this hypothesis ⁶³. There are also data indicating that resting progenitor cells may reside in the white matter awaiting reactivation.

Platelet-derived growth factors (PDGF), basic fibroblast growth factor (bFGF) and insulin-like growth factor (IGF-1) are mitogens which stimulate proliferation of O2A cells, an oligodendrocyte precursor identified in culture. These growth factors regulate the timing of oligodendrocyte development, proliferation, survival, migration, and myelin formation ^{32, 36, 42}.

- It has been shown that the establishment and maintenance of contact between a developing axon and oligodendrocyte process determines whether or axon will be myelinated ⁴⁶. There are two proposed signals initiating myelination, one of which is the diameter of an axon. The size of an axon reflects its level of maturation ¹³. The other is the electrical activity of an axon. For example, inhibition of optic nerve electrical activity with specific Na⁺ channel blocker tetrodotoxin prevents initiation of myelinogenesis in vitro and in vivo. Similarly, the myelinogenesis is enhanced by increasing electrical activity ^{30, 102}.

Successful remyelination depends on adhesion between the oligodendrocyte and axon. Oligodendrocytes receive an axonal signal that determines the myelin thickness. When the axons have reached their terminal size, this signal is never received again. It is clear both in vivo and in vitro that neurons influence myelination through the release of soluble factors and direct contact which plays an important role in oligodendrocyte differentiation and proliferation ⁶³. Other observations suggest the presence of an intrinsic program for myelin gene expression, which is independent of neuronal contact in that myelin is produced

when oligodendrocytes are cultured in vitro without neurons¹³. Thus, onset of myelination is a consequence of oligodendrocyte differentiation and maturation.

Regenerated myelin sheaths have common characteristics. The new internodes are abnormally short⁶⁵ and the new myelin sheath are thin with the myelin thickness to axonal diameter ratio decreased by as much as three fold.

Regenerated myelin sheaths have an otherwise normal lamellar periodicity^{39, 40, 64, 72, 73}.

1.8 Axon Regeneration

While it is clear that axons in the peripheral nervous system can regrow and successfully innervate targets, the possibility for this in central nervous system is not fully established. Whether the problem is one of complexity and failure to find a target, absence of appropriate stimuli, or failure of central neurons to attempt regrowth is not entirely clear^{31, 109}. However, it has been shown that injured central neurons can form growth cones in the adult brain⁸⁸. Expression of certain molecules, such as GAP-43, suggest that certain neurons may attempt to regrow.

Neuronal growth associated protein 43 (GAP-43, also identified as B50, F1, pp46 and neuromodulin) is a neuronal membrane phosphoprotein, which plays an important role in axonal growth related processes. It guides the growth of axons and their terminals, and modulates synaptic plasticity^{4, 98} and formation of new connections as demonstrated by long term potentiation^{5, 12}. Overexpression of

GAP-43 gene in transgenic mice results in the formation of aberrant connections and enhanced sprouting after brain injury ⁵.

During brain development, GAP-43 is produced at high levels at the time of neurite outgrowth and early stages of synaptogenesis. It declines sharply after mature connections have formed ^{8, 11}. However, neurons in specific brain regions with known plasticity do retain relatively high concentrations of GAP-43 for the functional and structural plasticity of these cell nerve terminals ^{8, 12}. When neurons are injured, the high levels of GAP-43 expression appears to be a characteristic feature in the neuronal regenerating process ^{29, 115}. In previous studies, a correlation between successful axonal regeneration and GAP-43 up-regulation have been found ^{7, 31, 103}. Thalamic neurons, which showed up-regulation of GAP-43 mRNA have a capacity to regenerate their axons ^{79, 108}. Cerebral ischemia in adult animals triggered a robust expression of GAP-43 ⁹⁹. However, other reports show that certain CNS neurons fail to increase GAP-43 following injury. In callosal axotomy experiments on adult mice, cortical neurons with callosal projections failed to upregulate GAP-43 mRNA ³⁵. Likewise sprouting axons in transected spinal cord do not appear to show increased GAP-43 protein ⁸¹. GAP-43 protein is enriched in axonal cones ^{3, 29, 55, 109}, and is involved in synthesis of membrane associated with the growth of various types of cellular processes, including those of microglial cells ¹¹⁰. GAP-43 is present not only in neurons, but also in O2A lineage cells in vitro ^{29, 110}. These cells are precursors of oligodendrocytes. In developing rat brain, GAP-43 is expressed by immature oligodendrocytes ¹⁷. Vaudano et al. (1995) ¹⁰⁸ using a more sensitive avidin-biotin-peroxidase method for an immuno-electron microscopic study,

visualized GAP-43 -like immunoreactivity in astrocyte processes. GAP-43 is down regulated during oligodendrocyte differentiation in both culture and developing rat brain. Finally, GAP-43 and myelination show an inverse expression pattern in the CNS ⁵⁴.

In vivo, GAP-43 is phosphorylated by protein kinase C (PKC) to become functionally active. This allows GAP-43 to respond to second messengers ⁵. GAP-43 interacts with secondary messenger systems to influence signal transduction in growth cones and the synaptic terminals via a calcium/calmodulin pathway ^{5, 54}. It is possible that phosphorylation enables GAP-43 to influence the organization of cytoskeleton proteins, as suggested by GAP-43 co-localization with cytoskeleton proteins and brain spectrin, as well as by in vitro binding assays ^{12, 70, 80}.

Although it has been proposed that developmental and regeneration-associated changes in GAP-43 synthesis is regulated at the level of transcription ³, it is also likely that the regulation of GAP-43 is determined by the rate of mRNA degradation ^{4, 82}, the translational efficiency ^{83, 87, 116}, and the post-translation modulation ⁵. Thus, the increased expression of GAP-43 may be one of prerequisites for axonal regeneration.

1.9 Summary

Hydrocephalus is a neurological disorder characterized by excessive cerebrospinal fluid (CSF) accumulation with enlarged ventricular cavities of the

brain. Progressive dilation of ventricles damages surrounding brain tissue by combination of the effects of mechanical injury, ischemic damage and accumulation of toxic metabolites.

One of the major pathological changes in hydrocephalus is damaged myelin and axons in the periventricular region. Hydrocephalus might affect myelin in two ways: 1. Specific or primary effects on myelin, which can delay myelination or damage myelin in absence of axonal injury. These changes are potentially reversible. 2. Effects on myelin secondary to axonal injury which is probably irreversible.

1.10 Hypotheses

We hypothesize that :

- 1. Hydrocephalus impairs myelination and axonal growth in the developing brain.**
- 2. Early treatment by shunting will allow retarded myelination to recover.**
- 3. Damaged axons might activate neurons to a state capable of enhancing survival or regeneration.**

In these experiments, we used kaolin-induced hydrocephalus in rats to study ultrastructural changes in periventricular white matter. The response of myelin proteolipid protein (PLP) and neuronal growth associated protein 43 (GAP-43) to hydrocephalic injury was tested.

2.0 Materials and Methods

All animals were treated in accordance with guidelines set forth by the Canadian Council on Animal Care. Three week old Sprague-Dawley rats (weight 43-61g) were divided into three groups. Group I : Hydrocephalus; Group II : Sham control; Group III : Shunted hydrocephalus. Group I and Group II rats underwent magnetic resonance (MR) imaging and were sacrificed immediately thereafter, either one week (H1, C1), two weeks (H2, C2) or four weeks (H4, C4) after treatment . Group III (H1S) rats underwent MR imaging at one week, were shunted, then they were killed three weeks after shunting. Numbers of rats in each group for each experiment are specified in the results section.

2.1 Induction of Hydrocephalus

Rats at three weeks age were anesthetized with ketamine/xylazine (90/10mg/kg) administrated i.m.. A 27 gauge needle was inserted into the cisterna magna, 0.05ml of sterile kaolin suspension (250mg) was injected slowly. Controls received sham injection of normal saline.

2.2 Magnetic Resonance Imaging

Rat brains were visualized by magnetic resonance imaging in a 7 Tesla Bruker Biospec/3 7T/21 cm horizontal bore spectrometer (Karlsruhe, Germany) with a radiofrequency coil surrounding the head. A coronal slice thickness of 1.0mm, TR of 3.0s, single echo TE of 80 msec were used to obtain T2-weighted images. Eight to ten contiguous coronal slices were obtained. Lateral ventricle size was assessed on the

slice which included the rostral third ventricle. Frontal ventricle size was expressed as a ratio determined by dividing the width of ventricle by the width of cerebrum.

2.3 Diversional Shunting of CSF

Immediately after MR imaging, a midline scalp incision was made and a 2mm diameter hole was drilled in the skull; 2mm lateral to the midline and 1mm posterior to the coronal suture. A sterile transparent silicone rubber tube with a right angle joint was placed into the right lateral ventricle to a depth of 4mm. When CSF flow was observed, the distal end of the tube was tunneled into the subcutaneous tissue of the back. The tube was anchored in place with cyanoacrylate glue and the incision was closed with polypropylene sutures.

2.4 Transmission Electron Microscopy

Twenty -one rats were killed by transcardiac perfusion of 2% paraformaldehyde and 1.5% glutaraldehyde in 0.12M phosphate buffer with 0.02mM CaCl_2 and 0.05M sucrose at pH 7.2 and 4°C. The brains were then removed and stored in the same fixative with 0.1% tannic acid added for 2-4 days at 4°C. Afterwards, samples of the corpus callosum were taken at the level of the anterior commissure. The tissue was post-fixed in 1% osmium tetroxide, and processed for embedding in Araldite/Epon. The specimens were cut so that the callosum was viewed in cross section and were complete from ependyma to the longitudinal cingulum fibers. Semi-thin sections (0.5 μm) were stained with toluidine blue and used to measure the thickness of the callosum in the midline one per animal.

Ultrathin sections were cut onto copper grids and stained with lead citrate and uranyl acetate. Sections were examined for evidence of structural damage to ependyma, axons, myelin, and specific features were photographed. Axons through all depths of the corpus callosum in true cross-sectional orientation were photographed at negative magnifications of 1500x and 4250x. These were chosen in the center of copper grid squares. For each animal five photographs were taken at each magnification. Final prints were enlarged 10x and the 15000x magnification prints were used to assess the relative number of myelinated axons using a B25 point counting grid with a square size of 4.6 x 4.6 cm¹¹¹. The 42500x magnification prints were used to assess the minimum axon diameter and the myelin thickness for all myelinated axons on the print. The myelin to axon ratio was determined for axons in different size ranges.

2.5 Northern Hybridization Analysis

Rats (n=32) were killed by decapitation and the brain was removed. The cerebrum was sliced coronally in 2mm thick pieces. The striatum, hippocampus, basal forebrain and diencephalon were removed. The samples included only cerebral cortex and white matter. The slice did not include the shunt insertion site. Total RNA was extracted from a slice of the parietal cerebrum following the method of GIBCO BRL instruction for TRIzol™ reagent. Simply, one slice of brain tissue (approximately 250mg) was put into 2ml TRIzol reagent and homogenized by a Polytron sonicator. RNA was separated into the aqueous phase by chloroform, and was precipitated by isopropanol. The concentrations of sample RNA were measured spectrophotometrically in water by light absorbance at 260 and 280 nm wavelength.

Then 10 µg of total RNA from each sample was electrophoresed in 1.2% agarose-formamide gel for three hours at 45 volts. Three µg of single strand RNA ladder (GIBCO BRL) was run in parallel as a molecular weight standard. The RNA fragments were transferred from the gel to positively charged nylon membrane (Boehringer Mannheim) with 20x SSC by upward capillary action. The RNA was immobilized by baking the blot at 80°C for 1.5 hours. RNA was stained with ethidium bromide, and the membrane was scanned for densitometric analysis of 28S band of RNA with a computerized scanner using image analysis software MCID M4 program.

The growth associated protein-43 (GAP-43) probe is a synthetic 30 mer oligonucleotides. The sequence 5'cagcttctttctcctcctcagcttggt3' is complementary to rat GAP-43 cDNA exon 2-3, extending from nucleotides 788-817 ⁹¹. The proteolipid protein (PLP) specific probe is a 30 mer oligonucleotide. The sequence of 5'tgtcgggatgtcctagccattttccaa3' is complementary to rat PLP cDNA, extending from nucleotides 546-575 ⁷⁴ at the 3' end of exon 3, and it recognizes a sequence not expressed in the related DM-20. The probes were 5'-digoxigenin conjugated and purified by gel electrophoresis (University of Calgary Core DNA Services). The probes were used for Northern hybridization and in situ hybridization. Control probes were sense strands. Sequences were checked to excluded homologies using the BLASTN program in the NCBI database ¹. The blots were prehybridized with 50% formamide, 1x Denhardt's solution, salmon sperm DNA (0.28mg/ml) and yeast tRNA (0.3mg/ml) hybridization solution at 50°C for 2-3 hours. Then the blots were rotated in the same hybridization solution with 600ng/ml GAP-43 probe or

150ng/ml PLP probe at 55°C overnight in Micro Hybridization Incubator Model 2000. The membranes were labeled with anti-digoxigenin antibody, Fab fragment conjugated to horseradish peroxidase (Boehringer Mannheim) in 1:5000 concentration followed by BM Chemiluminescence Blotting Substrate (POD) (Boehringer Mannheim). Then the membranes were exposed to Hyper X-ray film (Amersham), and were photographed using ethidium bromide stained 28S ribosomal RNA bands as loading control to normalize the target band density and analysis GAP-43 and PLP mRNA expression levels ³⁴.

2.6 In Situ Hybridization

A third set of rats (n=21) were sacrificed by overdose with pentobarbital followed by transcardiac perfusion with 3% paraformaldehyde in 0.1M phosphate buffer. The brains were removed and kept in the same fixative for one hour. Then the brain was cut into three coronal parts and stored in 30% sucrose for two days at 4°C, the brain was frozen in OCT embedding medium using methylbutane cooled by liquid nitrogen then stored at -80°C. Ten µm thick coronal sections from frontal lobe were cut and placed onto 3-aminopropyltriethoxysilane coated slides. The sections were prehybridized then covered with hybridization solution with GAP-43 probe or PLP probe in 3µg/ml concentration at 37°C overnight in an incubator. The sections were labeled with anti-digoxigenin antibody, Fab fragment conjugated with alkaline phosphatase, 1:1000 (Boehringer Mannheim) at 4°C overnight. Next, the sections were stained with NBT/BCIP detection system kit (Boehringer Mannheim) for two hours. The slides were examined for purple reaction products which showed the

distribution of GAP-43 mRNA and PLP mRNA in brain tissue. Negative controls included sense probe, sections incubated with no probe and sections pretreated with RNase.

2.7 Western Immunoblotting

The brains analyzed for mRNA were also analyzed for protein. A slice of frontal cerebrum was homogenized in RIPA buffer, the protein concentration was determined by Lowry method ⁶². The equal quantities of protein were loaded into 10% acrylamide/SDS gel and electrophoresed at 90 volts for 2 hours. Prestained molecular weight standard (Amersham Life Science) as run in parallel. Separated proteins were transferred to nitrocellulose membrane, and blocked in 5% milk. The membranes were incubated with mouse monoclonal anti-GAP-43 (Sigma), 1;1000 dilution, or rabbit polyclonal anti-PLP which recognizes a peptide sequence of PLP that is not found in the relative DM-20 protein (kindly provided by Dr. Wendy Macklin ³³) in 1:2000 concentration overnight at 4°C. Secondary antibodies were peroxidase-conjugated goat anti-mouse or anti-rabbit (Jackson ImmunoResearch laboratories) in 1:3000 concentration at room temperature for one hour. The target bands were visualized by chemiluminescence method, and densitometric readings were obtained.

2.8 Immunohistochemistry

Brains from one and three week hydrocephalic rats and controls were frozen and cut into 10 μ m thick sections onto gelatin coated slides. The sections of frontal

cerebrum were incubated with mouse monoclonal anti-GAP-43 (Sigma), 1:200, overnight at 4°C, followed by goat anti-mouse serum conjugated with Cy3 (Jackson ImmunoResearch Laboratories) in 1:350 concentration. Some slides were double labeled with rabbit polyclonal anti-myelin basic protein (Dako Corporation, USA), 1:10, followed by goat anti-rabbit serum conjugated with FITC (Jackson ImmunoResearch Laboratory) in 1:100 concentration. The intensity of GAP-43 immunoreactivity was assessed using spot light metering system of a Nikon Microphot FX epifluorescence microscope as an optical densitometer. The photometer reading used as measure of labeling intensity. Background labeling intensity over the ventricle was subtracted. An inverse function of the photometer reading was used as a measurement of labeling intensity. All brain sections were sampled in duplicate in the frontal cortex, supraventricular white matter next to lateral ventricle, adjacent subcortical white matter, and external capsule. This antibody did not work for immunohistochemistry under a variety of test conditions examined. The antibody was only useful for cell culture immunocytochemistry in the lab of origin.

2.9 Fluoro-Gold Tracer Pressure Injection

To assess efficiency of retrograde axonal transport across the corpus callosum, a fourth group of rats received an injection of 0.5-1.0 μ l of 4% Fluoro-Gold (Fluorochrome Inc., USA) into the frontal lobe, 2mm lateral and 1 mm posterior to the coronal suture, using a fine glass pipette attached to a microsyringe. Injection was made 1mm deep into the brain. Following injection, the incision was stapled. Two groups were studied. One group with Fluoro-Gold injection on the same day as

kaolin injection (n=7) and sham injection (n=2) were killed 14 days later. For the other group, Fluoro-Gold was injected 12 days after kaolin (n=6) and sham injection (n=3) and followed by sacrificed 4 days later. Rats were perfused with 3% paraformaldehyde in 0.1 M phosphate buffer. Fixed brains were removed and processed same as for immunohistochemistry. The retrogradely labeled neurons, which were in the lateral frontal cortex corresponding to cortical area 6 known to have connections through corpus callosum⁵⁰, were visualized with a Nikon Microphot FX epifluorescence microscope using a wide band UV excitation filter were counted in the contralateral cortex on four sections for each animal. The area of injection site was measured with Analyzed Micro Plan II Image Analysis System (Nikon Canada Inc.) to estimate efficiency of the tracer injection.

2.10 Data Analysis

All data were analyzed using StatView Version 4.1 (Abacus Concepts, Inc., Berkeley, CA). Z-score histograms were used to test the normal distribution. Unpaired t-tests were used to compare two groups. When there were three or more groups, ANOVA with posthoc Bonferroni-Dunn corrections were used.

3.0 Results

3.1 Ventricular Enlargement

One week after kaolin injection, many rats developed dome-like heads and they exhibited reduced weight gain. MR imaging confirmed dilation of the ventricles in these hydrocephalic brains. The degree of dilation increased with duration of hydrocephalus (Table 1, Figure 1).

Table 1. Size Index of Lateral Ventricles (a)

Time After Injection	Control	Hydrocephalus	Shunt
1 week	0.001 ± .001 (n=6)	0.426 ± .036 * (n=10)	
2 week	0.002 ± .002 (n=5)	0.450 ± .040 * (n=10)	
4 week	0.010 ± .008 (n=9)	0.643 ± .049 * (n=15)	0.474 ± .040 ** (n=12)

(a) Data are expressed as mean ± SEM by dividing the width of frontal horns of lateral ventricle by width of cerebrum at the same MR image level.

* p < 0.001 vs. control; ** p < 0.001 vs. H4

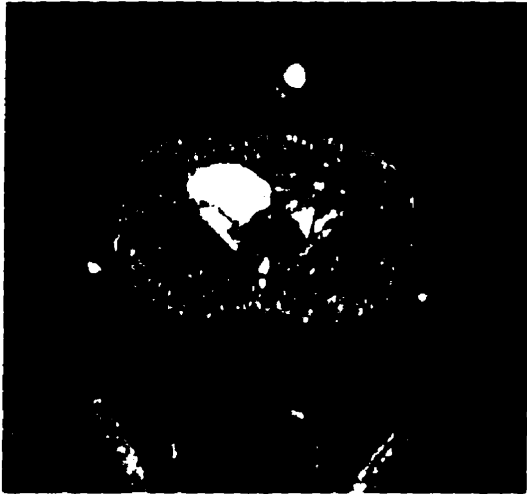
Hydrocephalic rats had lower body weights than controls. Whereas shunted rats had weights similar to controls. The ventricles of the shunted rats showed variable reductions in size, but never returned to normal. Histological examination showed that in hydrocephalic rats, kaolin filled macrophages were identified throughout the basal subarachnoid space. As the ventricles dilated, the septal region became elongated and ultimately separated from the displaced corpus callosum. The

Figure 1

Magnetic resonance T2-weighted images of frontal lobes of rat brain. The upper panels show two coronal slices through a hydrocephalic rat brain, one week after kaolin injection (H1). The enlarged lateral ventricles and third ventricle appear white. The rat was shunted immediately after obtaining these images. The lower panels show two comparable coronal slices from the same rat, three weeks after shunting (H1S). The lateral and third ventricles are reduced in size, albeit asymmetrically. Signal intensity in the external capsule has normalized indicating resolution of the edema.



PRESHUNT (H1)



POSTSHUNT (H1S3)

corpus callosum which was thinner. Corpus callosum thickness was determined on tissue prepared for electron microscopy. The thickness of corpus callosum in 4 week hydrocephalus is thinner than in controls, and significantly thinner compared with same age shunted rats (Table 2).

Table 2. Corpus callosum thickness (mm) (a)

Shunted	Control	Hydrocephalic	Shunted
1 week	0.26 ± .01 (n=2)	0.24 ± .08 (n=2)	
2 week	0.26 ± .01 (n=2)	0.25 ± 0.01 (n=2)	
4 week	0.29 ± .03 (n=2)	0.15 ± .06 (n=5)	0.35 ± .09 * (n=2)

(a). Values (mean ± SEM) were determined by measuring thickness of the corpus callosum (mm) in plastic embedded sections at the level of the anterior commissure.
* p<0.05 vs. 4 week hydrocephalus.

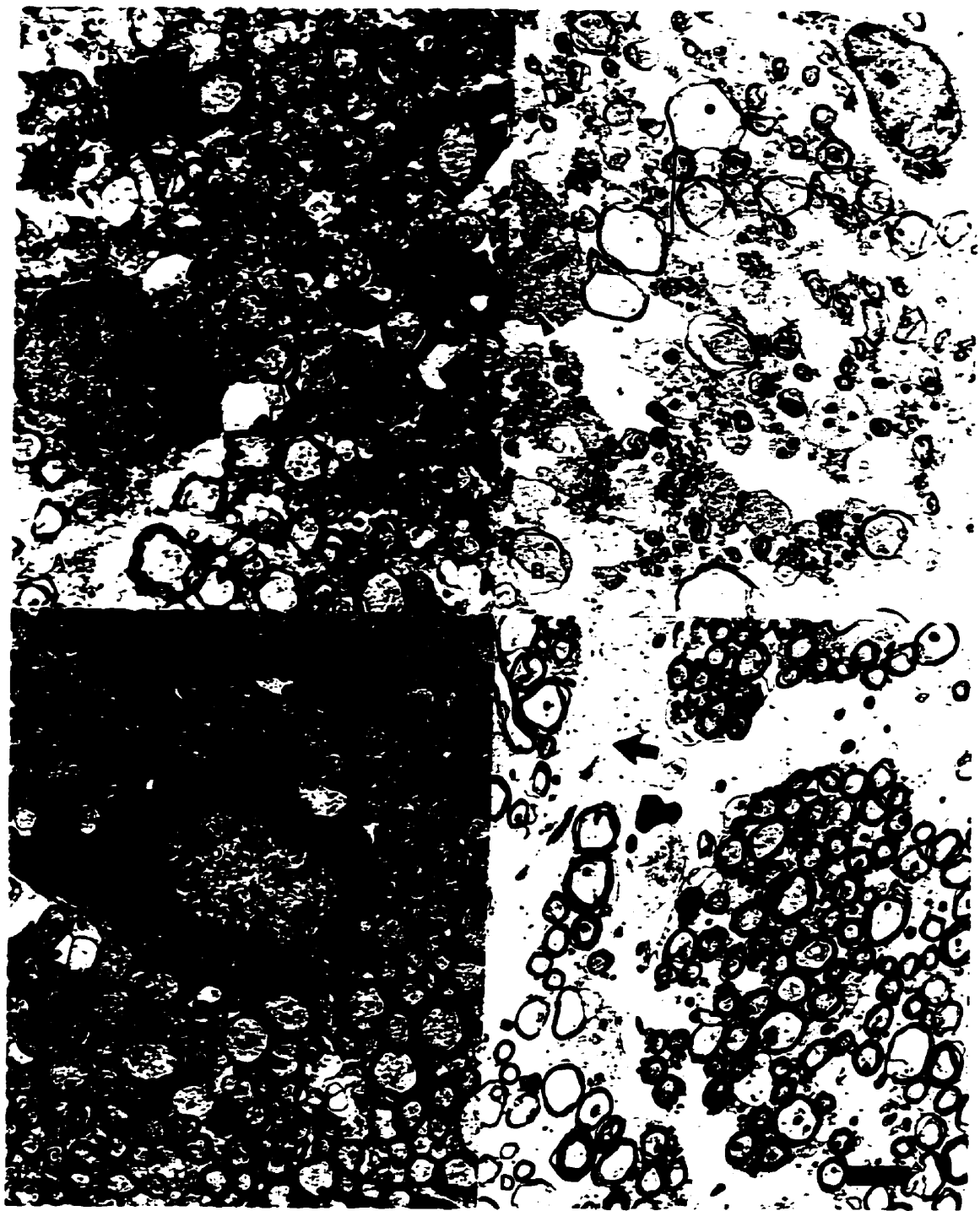
3.2 Ultrastructure of Corpus Callosum

Myelin sheaths in control rats had normal configuration. Astrocytes and oligodendrocytes showed normal morphology. Ependymal cells were intact with microvilli and cilia. The proportion of myelinated axons increased with age.

In one week hydrocephalic rats, a wide range of axons were unmyelinated. The axons were dispersed and the astrocyte processes were swollen, suggestive of periventricular edema. Although the oligodendrocytes were intact, the endoplasmic reticulum was distended, the myelin thickness seemed less than in controls (Figure 2).

Figure 2

Transmission electron micrographs showing representative areas of corpus callosum at different stages in rat development and hydrocephalus progression. Panel A shows an oligodendrocyte (o) among myelinated and unmyelinated axons in a C1 control rat. Panel B shows a comparable H1 hydrocephalic rat sample with dispersed, thinly myelinated axons (long arrow) and enlarged extracellular spaces. The rough endoplasmic reticulum (arrowhead) in the oligodendrocytes is distended. Panel C shows a dense collection of well myelinated axons surrounding an oligodendrocyte (o) in a C4 control rat. Panel D shows well myelinated axons divided into clusters by reactive astrocyte processes (arrow) in a hydrocephalic rat that had been shunted early (H1S). All micrographs same magnification, Bar = 1 μ m.



In two week hydrocephalic rats, the myelin thickness had increased, swollen axons were found easily, reactive astrocytes were obvious and there was severe ependymal destruction. The oligodendrocytes looked similar to those in controls.

In four week hydrocephalic rats, the majority of larger axons were myelinated, but there was widespread axonal damage and ependymal loss with profound reactive astrogliosis and microglial cell enlargement. The myelin and oligodendrocytes that were present appeared to be intact. Shunted rats also exhibited reactive gliosis (Figure 2) and scattered swollen axons (Figure 3).

The number of myelinated axons per unit area of corpus callosum increased with age, peaking in the C4 group, at an age of 7 weeks. Hydrocephalic rats had fewer myelinated axons per unit area at all stages. Early shunting prevented the loss of myelinated axons and the number of myelinated axons per unit area was inversely related to the size of the lateral ventricles ($r = -0.625$) (Table 3).

Table 3. Electron Microscopic Determination of Axons / Unit Area in Corpus Callosum Cross Sections

Shunted	Control (a)	Hydrocephalic	Shunted
1 week	35.8 ± 1.6 (n=1)	18.5 ± 1.7 * (n=2)	
2 week	39.8 ± 1.5 (n=1)	28.9 ± 2.0 (n=2)	
4 week	54.2 ± 2.3 (n=1)	39.0 ± 1.6 ** (n=7)	53.5 ± 2.4 (n=2)

(a). Relative quantity of myelinated axons/unit area. Values (mean ± SEM) were determined by counting myelinated axons intersecting points on a counting grid, as described in the Methods 2.4. Therefore the numbers are only relative values and are without units.

* $p < 0.001$ Vs. 1 week control; ** $p < 0.0001$ vs. 4 week control and vs. shunted.

Figure 3

Electron micrograph showing part of the corpus callosum of a 4 week hydrocephalic rat. A damaged axon is swollen and full of organelles.



A total 2795 myelinated axons were measured to determine the myelin thickness to axon diameter ratio. In the C1 controls a wide size range of axons were unmyelinated. Among axons less than or equal to 0.2 μm diameter (n=645), there was an age-related decline in the myelin thickness ratio. There were no difference between control and hydrocephalic rats (data not shown). Among axons between 0.2 and 0.4 μm diameter (n=1489), the mean myelin thickness ratio was 0.134 for all control ages. There were no significant age - or treatment-related differences (data not shown). Among axons greater than 0.4 μm diameter (n=625), the relative myelin thickness decreased slightly with age²⁸, and was significantly reduced in the H1 hydrocephalus group. Shunted rats showed axon quantity and myelin thickness similar to controls (Table 4).

Table 4. Ratio of Myelin Thickness to Axon Diameter for Myelinated Axons in the Corpus Callosum Greater Than 0.4 μm Diameter (a)

Time After Injection	Control	Hydrocephalic	Shunted
1 week	0.125 \pm .028 (n=1)	0.050 \pm .008 * (n=2)	
2 week	0.096 \pm .006 (n=1)	0.081 \pm .007 (n=2)	
4 week	0.102 \pm .004 (n=1)	0.106 \pm .005 (n=7)	0.086 \pm .004 (n=2)

(a) mean \pm SEM, n values are the number of animals used

* p<0.0001 vs. 1 week control.

3.3 PLP mRNA and Protein

In situ hybridization of control brains demonstrated that PLP mRNA was located in white matter cells whose morphology was consistent with

oligodendroglial identity (Figure 4). In early hydrocephalus, the distribution of cells was apparently normal, but in severely hydrocephalic rats it was difficult to find labeled cells in very thinned corpus callosum. We did not attempt to quantitatively assess the level of mRNA in these preparations.

Northern hybridization results showed PLP mRNA in early hydrocephalic rats was increased although it was not statistically significant. In the four week hydrocephalic group, the mRNA was significantly lower than in controls. This decrease was partially prevented in the shunted group (Table 5, Figure 5).

Table 5. PLP mRNA Expression Levels (a)

Time After Injection	Control	Hydrocephalic	Shunted
1 week	119.8 ± 8.1 (n=3)	152.9 ± 16.3 (n=6)	
2 week	92.1 ± 38.5 (n=4)	144.7 ± 52.9 (n=6)	
4 week	142.1 ± 40.6 (n=4)	55.3 ± 7.0 * (n=4)	96.5 ± 14.8 (n=5)

(a) arbitrary densitometric units expressed as mean ± SEM. The different age groups are not directly comparable, because they were processed separately.

* P < 0.05 vs. C4.

PLP protein was lower in one week and four week hydrocephalic rats than in controls. Shunting prevented the reduction in the four week hydrocephalic rats to some extent (Table 6, Figure 6).

Figure 4 (upper two panels)

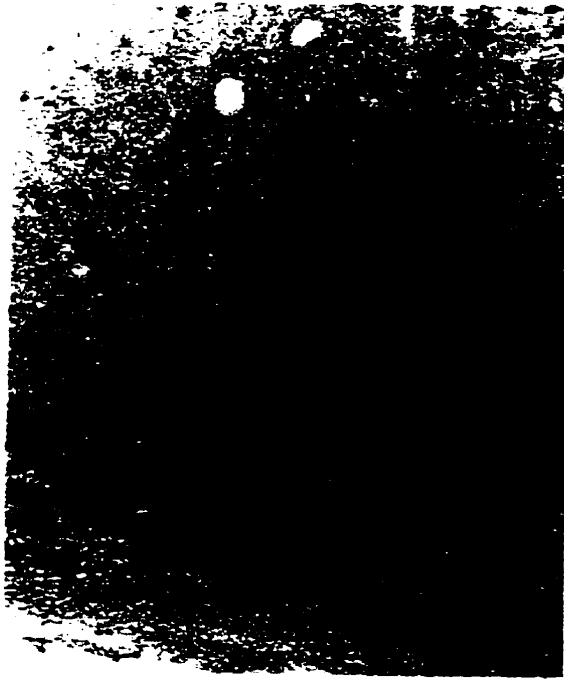
In situ hybridization showing localization of the mRNA for proteolipid protein (PLP) to cells in the supraventricular white matter of a rat that had been hydrocephalic for two weeks. Very little signal is seen in the adjacent cortex and there is no background reaction product over the ventricle. The panel on the right shows an adjacent negative control slide pretreated with RNase. Bar = 100 μ m.

Figure 5 (bottom left panel)

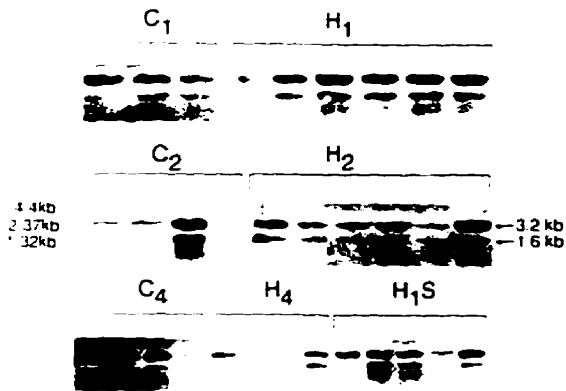
Photograph of Northern blots showing the mRNA for proteolipid protein (PLP) in samples from control (C) and hydrocephalic (H) rat cerebrum. Bands are evident at 3.2 and 1.6 kb sizes as would be expected. Positions of size markers are shown on the left of the middle set. Refers to Table 5 for densitometric analysis which showed that the levels of PLP mRNA in one and two week hydrocephalic brains (H1 and H2) are slightly greater than in comparable controls (C1 and C2). The levels in the 4 week hydrocephalic brains (H4) are significantly less than in controls (C4) and shunted brains (H1S).

Figure 6 (bottom right panel)

Representative immunoblot showing proteolipid protein (PLP) in samples from 2 week control (C2) and 2 week hydrocephalic (H2) rat cerebrum. Expected band(s) at about 25kD molecular weight are evident. The 31 kD size marker is shown on the left. Refers to Table 6 which showed that the protein expression levels are similar in the two groups.



PLP mRNA



Proteolipid Protein (PLP) Immunoblot

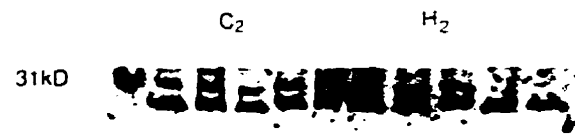


Table 6. PLP Protein Levels in Western Immunoblotting (a)

Time After Injection	Control	Hydrocephalus	Shunt
1 week	1.75 ± .20 (n=3)	0.57 ± .16 * (n=6)	
2 week	1.20 ± .11 (n=4)	0.75 ± .20 (n=6)	
4 week	1.14 ± .31 (n=4)	0.33 ± .08 **(n=4)	0.58 ± .22 (n=5)

(a) arbitrary densitometric units expressed as mean ± SEM. The different age groups are not directly comparable, because they were processed separately.

* p< 0.001 vs. C1. ** p<0.05 vs. C4.

3.4 GAP-43 mRNA and Protein

The GAP-43 probe specifically recognized GAP-43 mRNA mainly located in neuron cell bodies of cortex and hippocampus (Figure 7). Hydrocephalic and control rats exhibited similar distribution of GAP-43 mRNA positive cells. Both groups showed an age-related decrease. Rarely were cells in white matter labeled.

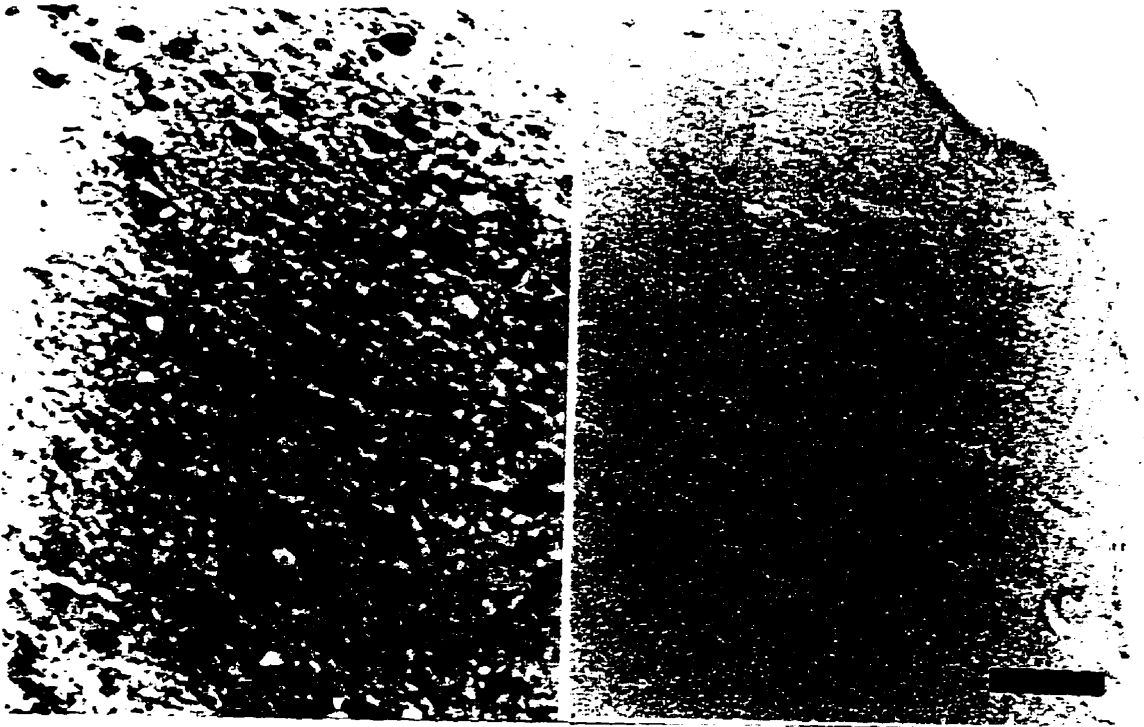
In the one week hydrocephalic group, GAP-43 mRNA was significantly increased compared with controls. This trend persisted at two weeks, but in the four week group, the mRNA had decreased slightly in both hydrocephalic and shunted rats (Table 7, Figure 8).

Figure 7 (upper panels)

Photomicrograph showing localization by in situ hybridization of GAP-43 mRNA in neurons of the cerebral cortex of a control rat, one week after sham injection. On the right is a control slide that was subjected to RNase digestion prior to hybridization. Bar = 50 μ m

Figure 8 (lower panel)

Photograph of representative Northern blot hybridization membranes showing GAP-43 mRNA in cerebrum homogenates from control (C), hydrocephalic (H) rats at 1, 2, or 4 weeks after kaolin injection, and shunted hydrocephalic (H1S) rats. Location of size markers are shown on the left. The mRNA band lies at the predicted size of 1.5kb. Referes to Table 7 which showed that the level of GAP-43 mRNA in one week hydrocephalic rats (H1) is greater than in comparable controls (C1). This trend persisted at two weeks, but in the four week group, the mRNA had decreased slightly in both hydrocephalic and shunted rats.



GAP43 mRNA

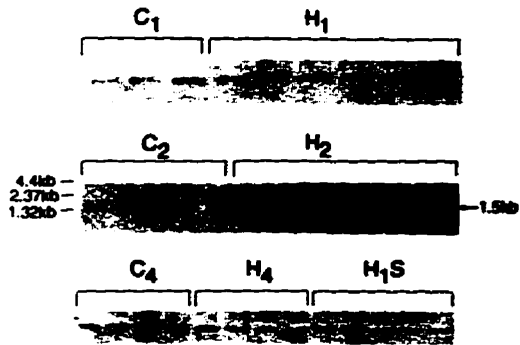


Table 7. GAP-43 mRNA Expression Levels (a)

Time After Injection	Control	Hydrocephalic	Shunted
1 week	73.5 ± 8.6 (n=3)	104.0 ± 4.9 *(n=6)	
2 week	95.6 ± 9.9 (n=4)	111.0 ± 13.9 (n=4)	
4 week	111.0 ± 14.4(n=4)	90.8 ± 3.5 (n=4)	97.0 ± 8.1 (n=5)

(a) arbitrary densitometric units expressed as mean ± SEM

* P< 0.05 vs. C1.

In the early stages of hydrocephalus (H1 and H2), GAP-43 protein levels were slightly lower than same age controls as revealed by immunoblot. In the four week hydrocephalic rats, the protein was significantly increased. Shunted rats had the protein level intermediate between control and hydrocephalus (Table 8, Figure 9).

Table 8. GAP-43 Protein Levels in Western Immunoblotting (a)

Time After Injection	Control	Hydrocephalic	Shunted
1 week	2.07 ± .12 (n=3)	1.83 ± .14 (n=6)	
2 week	1.92 ± .08 (n=4)	1.56 ± .09 (n=6)	
4 week	1.56 ± .21 (n=4)	2.04 ± .05 *(n=4)	1.83 ± .14 (n=5)

(a) arbitrary densitometric units expressed as mean ± SEM.

* P<0.05 vs. C4

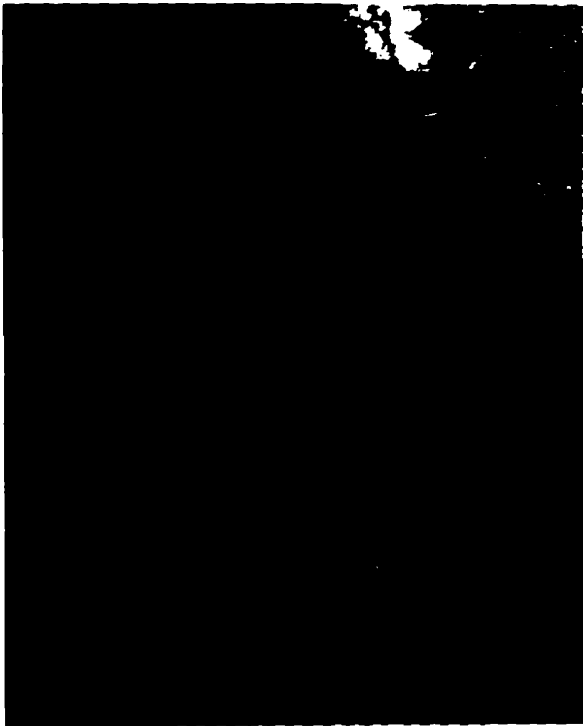
Immunohistochemical labeling of GAP-43 in control brains was detected diffusely in the cortical and striatal neuropil. Labeling in the white matter was minimal. In hydrocephalic rats, a distinct band of intense labeling was seen in the white matter immediately adjacent to the ventricle (Figure 10), but not in the subcortical white matter or external capsule. Fluorescence intensity was measured in

Figure 9 (bottom right panel)

Photograph of representative Western blot membranes showing GAP-43 protein in cerebrum homogenates from hydrocephalic rats one week after kaolin injection (H1) and comparable controls (C1). Location of the 46kD molecular size marker is shown on the left. Refer to Table 8 which showed that the protein levels are similar in the two groups.

Figure 10

Fluorescence photomicrographs showing GAP-43 localization in the cerebral white matter. Upper left panel shows intense labeling in the periventricular white matter, one week following induction of hydrocephalus. In some regions a linear pattern suggestive of axonal localization is evident. Upper right panel shows a comparable control brain with minimal immunofluorescence in white matter and slightly more intense labeling in the nearby striatum. Lower left panel shows a negative control processed without the primary antibody of a hydrocephalic brain at the gray white matter junction. Bar = 50 μ m for all plates.



Growth associated Protein (GAP) 43 antibody

C.

H.

46kD -



cortex white matter adjacent to the ventricle, subcortical white matter, and external capsule. In one week and three week hydrocephalic, significantly higher intensity was found in the periventricular white matter. In cortex, the intensity was slightly higher than controls (Table 9).

Table 9 . GAP-43 Immunohistochemistry Intensity (a)

Treatment Groups	Frontal cortex	Periventricular white matter	Subcortical white matter	External capsule
C1(n=3)	1.7 ± .7	2.3 ± .7	1.6 ± .1	0.7 ± .3
H1(n=4)	2.8 ± .6	4.6 ± 1.6 *	1.8 ± .3	0.9 ± .2
C3(n=4)	1.6 ± .4	2.0 ± .3	1.7 ± .1	0.7 ± .3
H3(n=4)	2.5 ± .3	3.7 ± .6 *	1.8 ± .3	0.6 ± .1

(a) arbitrary units of relative immunofluorescence intensity, mean ± SEM
 * P<0.05 vs. Control

3.5 Retrograde Neuronal Labeling

Fluoro-Gold tracer retrogradely labeled neuron cell bodies yielding fine granules of whitish fluorescence under ultraviolet excitation. Injection site areas were variable in size as defined by locally labeled cells. Retrogradely labeled neurons in the contralateral cortex were counted on four sections. To account for variable injection between animals, a ratio was calculated by dividing the numbers of labeled neurons by the injection area. Injection efficacy varied because of reflux from the injection site. Labeled cells could be seen in subarachnoid space. The numbers of labeled neuron cells were similar in two groups, and there was no relation to ventricular size in either group (Table 10). Thus, there was no significant damage of axonal transport across the corpus callosum in the two week hydrocephalic rats.

Table 10. Labeled Neuron Cells / Injection Area (a)

	Ventricular size	Labeling index
Labeled at day 0		
Control	0.01	$0.73 \pm .12$ (n=3)
Hydrocephalic	0.35	$1.08 \pm .10$ (n=6)
Labeled at day 12		
Control	0.01	$0.17 \pm .06$ (n=3)
Hydrocephalic	0.30	$0.48 \pm .10$ (n=6)

(a) . Data are expressed as mean \pm SEM

4.0 Discussion

Hydrocephalus progressively damages periventricular white matter. Much work indicates that axons are the primary structure to be damaged ²⁴, but there are also some data in immature cats indicating that myelin might be primarily affected in the developing brain ⁹. The three week old rats used in our experiments are at a developmental stage when myelination peaks (19-25 days) ⁶⁰. Their brain development stage is roughly comparable to that of humans during the first year ¹⁰⁷ when hydrocephalus is the most prevalent ⁷⁸. In these experiments, morphological and molecular methods were used to study white matter damage in the immature rat brain. We also looked for evidence that the changes could be reversed by surgical treatment of the hydrocephalus.

PLP is a major myelin structural protein, it functions in compaction of the intraperiod line of myelin. A smaller isoform of PLP, DM-20, is an alternative splicing PLP gene transcript product. It is a non-myelin protein related somehow to brain development ^{6, 105}. Both our antibody and probe were directed against the portion of PLP not expressed in DM-20. In one week hydrocephalic rats, myelin around axons with diameter greater than 0.4 μm was significantly thinner and myelin protein PLP content was reduced, but there was little evidence for gross loss of white matter or ultrastructural damage to axons. Electron micrographs demonstrated periventricular white matter edema with dispersed axons. This may be a factor causing the apparent decrease in axon numbers per unit area. The thinning

of the myelin sheaths likely represents impaired myelination. Reduced activity of ceramide galactosyltransferase enzyme (CGaT), an enzyme active in myelinating oligodendrocytes, and reduced myelin basic protein content (MBP) in related experiments support the idea that early myelination was impaired ²⁸. The possible mechanism could be a metabolic factor affecting oligodendrocytes. This may be caused by a diffusible factor released from reactive astrocytes ²⁸, or from damaged ependyma ²², or a toxic effect from accumulating metabolites that would normally be eliminated by outflow of CSF ²³. Elevated PLP mRNA during the first week suggests that oligodendrocytes are programmed to express PLP gene actively and may be attempting, but failing, to produce normal amount of the myelin protein. Another possible cause of delayed myelination is a consequence of altered axonal activity. Axon-glia cell interaction is a requirement for myelination. Axonal signaling molecules and electrical activity can act directly on oligodendrocytes to trigger myelination ¹⁵. Impaired function or impulse transmission along stretched axons in the hydrocephalic brain might down-regulate oligodendrocyte activity ².

In the two week hydrocephalic group, PLP protein levels increased to become comparable to controls, myelin thickness increased, and PLP mRNA expression was increased. As the hydrocephalus progressed, severe injury to myelin and axons were observed. These rats exhibited thin corpus callosum, reduced quantity of myelinated axons, degenerated axons, depletion of PLP mRNA and protein, decreased activity of myelin enzyme p-nitrophenylphosphorylcholinephosphodiesterase (PNPPP), and reduced MBP ²⁸. Surviving axons, however, eventually developed normal myelin sheaths.

Shunt treatment after one week of hydrocephalus was associated with reduced ventricular size and increased animal weights. Early shunting was associated with recovery of myelin, according to ultrastructural features, molecular content of PLP and MBP, and enzyme activities²⁸. This suggests that either oligodendrocytes were impaired but then allowed to recover, or that new oligodendrocytes aided myelin production.

GAP-43 is generally considered to be a protein related to neuronal regeneration and synaptogenesis; it plays a role in synaptic plasticity and formation of new connections^{5, 12}. Previous studies supported the hypothesis that there is a close relationship between up-regulated expression of GAP-43 and axonal regeneration^{5, 7, 31, 79}. GAP-43 protein in periventricular white matter in one week hydrocephalic rats is increased greatly, corresponding to elevated cerebral mRNA. In frontal cortex, GAP-43 immunoreactive intensity was only slightly higher than control. One explanation for local periventricular increase in GAP-43 protein is expression in glial cells, as it has been shown that GAP-43 is expressed in O2A oligodendrocyte progenitor cells and astrocytes^{29, 110}. However, the pattern of immunoreactivity was more suggestive of axonal rather than cell body location. Other work in the laboratory confirmed axonal localization by immunoelectron microscopy. Furthermore, we failed to show any significant number of GAP-43 mRNA containing cells in the periventricular region at any time point. Neuronal injury will induce GAP-43 synthesis and the protein is subsequently fast transported along axons⁹⁵. In the hydrocephalic condition, periventricular white matter is affected most severely²⁴. It is possible that transported GAP-43 could come to the

injured periventricular axons, but be blocked there and fail to be transported further. As a result, the periventricular axons exhibited the strongest intensity of GAP-43-like immunolabeling. Although no obvious impairment of axonal transport was evident on the Fluoro Gold tracer study, some swollen axons indicative of damage were identified at the electron microscope level.

Total GAP-43 protein as measured in immunoblots of the cerebrum was elevated in only late hydrocephalus. Delayed accumulation of GAP-43 protein has previously been shown as long as 1-2 weeks following increased mRNA expression^{16, 94}. However, because the immunoblots displayed total amount of GAP-43 protein from cortex and white matter, the slight local periventricular increase was not represented in early stage. The deposition and stabilization GAP-43 protein can be regulated by local post-translational modification, such as phosphorylation^{16, 94}. However, it should noted that we observed no significant shift in molecular weight in our immunoblot experiment. The reactive GAP-43 mRNA and protein increase implies that neurons underwent compositional changes that could prepare them for regeneration of injured axons. Stretching of neuron cell processes in culture also promotes growth of the processes in the absence of injury⁴⁵. Thus the stimulus may be an exaggerated growth response that precedes actual injury. Enhanced GAP-43 expression, it should be noted, is not always accompanied by axonal regeneration, it also depends on a permissive environment in the area of a lesion and the ability of peripheral factors or influences reaching neuron cell body^{31, 109}.

In conclusion, early hydrocephalus caused a delay in periventricular myelination in the neurologically immature rat brain. This delay could be reversed

by early, but not late-shunt treatment. Neuronal cells increased GAP-43 mRNA at 1 and 2 weeks and production of GAP-43 protein at 4 weeks as a response to hydrocephalic brain injury. Accumulation of GAP-43 was especially pronounced in periventricular axons which were also shown to be susceptible to damage. Whether elevated GAP-43 accompanies axonal regeneration following shunting or if it represents an enhanced survival mechanism needs further study.

5.0 References

1. Altschul S.F., Gish W., Miller W., Myers E.W. and Lipman D.J. (1990) Basic local alignment search tool. *J. Molec. Biol.* **215**, 403-410.
2. Barres B.A. and Raff M.C. (1993) Proliferation of oligodendrocyte precursor cells depends on electrical activity in axons. *Nature* **361**, 258-260.
3. Basi G., Jacobson R.D., Virag I., Schilling J. and Skene J.H.P. (1987) Primary structure and transcriptional regulation of GAP-43, a protein associated with nerve growth. *Cell* **49**, 785-791.
4. Benowitz L.I. and Perrone-Bizzozero N.I. (1991) The expression of GAP-43 in relation to neuronal growth and plasticity: when, where, how, and why? *Prog. Brain Res.* **89**, 69-87.
5. Benowitz L.I. and Routtenberg A. (1997) GAP-43: an intrinsic determinant of neuronal development and plasticity. *Trends Neurosci.* **20**, 84-91.
6. Campagnoni A.T. (1995) Molecular biology of myelination. In *Neuroglia* (ed. Kettenmann H. and Ransom B.R.), Vol. pp. 555-570. Oxford University Press, New York.
7. Campbell G., Anderson P.N., Turmaine M. and Liebermann A.R. (1991) GAP-43 in the axons of mammalian CNS neurons regenerating into peripheral nerve grafts. *Exp. Brain Res.* **87**, 67-74.
8. Chao S., Benowitz L.I., Krainc D. and Irwin N. (1996) Use of a two-hybrid system to investigate molecular interactions of GAP-34. *Mol. Brain Res.* **40**, 195-202.
9. Chumas P.D., Drake J.M., Del Bigio M.R., Da Silva M. and Tuor U.I. (1994) Anaerobic glycolysis preceding white-matter destruction in experimental neonatal hydrocephalus. *J. Neurosurg.* **80**, 491-501.
10. Clark R.G. and Milhorat T.H. (1970) Experimental hydrocephalus: Part 3. Light microscopic findings in acute and subacute obstructive hydrocephalus in the monkey. *J. Neurosurg.* **32**, 400-413.
11. Clayton G.H., Mahalik T.J. and Finger T.E. (1994) Expression of GAP43 mRNA in normally developing and transplanted neurons from the rat ventral mesencephalon. *J. Comp. Neurol.* **347**, 470-480.
12. Coggins P.J. and Zwiers H. (1991) B-50 (GAP-43): biochemistry and functional neurochemistry of a neuron-specific phosphoprotein. *J. Neurochem.* **56**, 1095-1106.
13. Colello R.J., Devey L.R., Imperato E. and Pott U. (1995) The chronology of oligodendrocyte differentiation in the rat optic nerve: Evidence for a signaling step initiating myelination in the CNS. *J. Neurosci.* **15**, 7665-7672.
14. Collins P. (1979) Experimental obstructive hydrocephalus in the rat: A scanning electron microscopic study. *Neuropathol. Appl. Neurobiol.* **5**,
15. Cook J.L., Irias-Donaghey S. and Deininger P.L. (1992) Regulation of rodent myelin proteolipid protein gene expression. *Neurosci. Lett.* **137**, 56-60.
16. Costello B., Lin L.H., Meymandi A., Bock S., Norden J.J. and Freeman J.A. (1991) Expression of the growth- and plasticity-associated neuronal protein, GAP-43, in PC12 pheochromocytoma cells. *Prog. Neurobiol.* **89**, 47-67.
17. Curtis R. (1993) Growth-associated protein-43 (GAP-43) is expressed by glial cells of the central and peripheral nervous system. *An. N. Y. Acad. Sci.* **679**, 407-411.
18. Curtis R., Hardy R., Reynolds R., Spruce B.A. and Wilkin G.P. (1991) Down-regulation of GAP-43 during oligodendrocyte development and lack of expression by

- astrocytes in vivo: implications for macroglial differentiation. *Eur. J. Neurosci.* 3, 876-886.
19. da Silva M.C., Michowicz S., Drake J.M., Chumas P.D. and Tuor U.I. (1995) Reduced local cerebral blood flow in periventricular white matter in experimental neonatal hydrocephalus - restoration with CSF shunting. *J. Cereb. Blood Flow Metab.* 15, 1057-1065.
20. Dandy W.E. and Blackfan K.D. (1913) An experimental and clinical study of internal hydrocephalus. *JAMA* 61, 2216-2217.
21. De Feo D.R., Myers P., Foltz E.L., Everett B. and Ramshaw B. (1979) Histological examination of kaolin-induced hydrocephalus. Its implications in the therapy of animals with experimentally induced hydrocephalus. *J. Neurosurg.* 50, 70-74.
22. Del Bigio M.R. (1995) The ependyma: a protective barrier between brain and cerebrospinal fluid. *Glia* 14, 1-13.
23. Del Bigio M.R. (1989) Hydrocephalus-induced changes in the composition of cerebrospinal fluid. *Neurosurgery* 25, 416-423.
24. Del Bigio M.R. (1993) Neuropathological changes caused by hydrocephalus. *Acta Neuropathol.* 85, 573-585.
25. Del Bigio M.R. and Bruni J.E. (1988) Changes in periventricular vasculature of rabbit brain following induction of hydrocephalus and after shunting. *J. Neurosurg.* 69, 115-120.
26. Del Bigio M.R. and Bruni J.E. (1988) Periventricular pathology in hydrocephalic rabbits before and after shunting. *Acta Neuropathol.* 77, 186-195.
27. Del Bigio M.R., da Silva M.C., Drake J.M. and Tuor U.I. (1994) Acute and chronic cerebral white matter damage in neonatal hydrocephalus. *Can. J. Neurol. Sci.* 21, 299-305.
28. Del Bigio M.R., Kanfer J.N. and Zhang Y.W. (1997) Myelination delay in the cerebral white matter of immature rats with kaolin-induced hydrocephalus is reversible. *J. Neuropathol. Exp. Neurol.* 56, 1053-1066.
29. Deloulme J.-C., Janet T., Au D., Storm D.R., Sensenbrenner M. and Baudier J. (1990) Neuromodulin (GAP43): a neuronal protein kinase C substrate is also present in O-2A glial cell lineage. Characterization of neuromodulin in secondary cultures of oligodendrocytes and comparison with the neuronal antigen. *J. Cell Biol.* 111, 1559-1569.
30. Demerens C., Stankoff B., Logak M., Anglade P., Allinquant B., Couraud F., Zalc B. and Lubetski C. (1996) Induction of myelination in the central nervous system by electrical activity. *Proc. Natl. Acad. Sci. USA* 93, 9887-9892.
31. Doster S.K., Lozano A.M., Aguayo A.J. and Willard M.B. (1991) Expression of growth associated protein GAP-43 in adult rat retinal ganglion cells following axonal injury. *Neuron* 6, 635-647.
32. Dubois-Dalcq M. and Armstrong R. (1990) The cellular and molecular events of central nervous system remyelination. *BioEssays* 12, 569-576.
33. Duchala C.S., Asotra K. and Macklin W.B. (1995) Expression of cell surface markers and myelin proteins in cultured oligodendrocytes from neonatal brain of rat and mouse: a comparative study. *Dev. Neurosci.* 17, 70-80.
34. Duhl D.M., Gillespie D.D. and Sulser F. (1992) Ethidium bromide fluorescence of 28S ribosomal RNA can be used to normalize samples in Northern or dot blots

- when analyzing small drug-induced changes in specific mRNA. *J. Neurosci. Meth.* 42, 211-218.
35. Elliot E.J., Parks D.A. and Fishman P.S. (1997) Effect of proximal axotomy on GAP-43 expression in cortical neurons in the mouse. *Brain Res.* 755, 221-228.
36. Ellison J.A., Scully S.A. and de Vellis J. (1996) Evidence for neuronal regulation of oligodendrocyte development: cellular localization of platelet-derived growth factor a receptor and a-chain mRNA during cerebral cortex development in the rat. *J. Neurosci. Res.* 45, 28-39.
37. Fishman R.A. and Greer M. (1963) Experimental obstructive hydrocephalus. Changes in the cerebrum. *Arch. Neurol.* 8, 156-161.
38. Gardinier M.V. and Macklin W.B. (1988) Myelin proteolipid protein gene expression in jimpy and jimpymsd mice. *J. Neurochem.* 51, 360-369.
39. Gledhill R.F., Harrison B.M. and McDonald W.I. (1973) Pattern of remyelination in the CNS. *Nature* 244, 443-444.
40. Gledhill R.F. and McDonald W.I. (1977) Morphological characteristics of central demyelination and remyelination - a single-fiber study. *Ann. Neurol.* 1, 552-560.
41. Gopinath G., Bhatia R. and Gopinath P.G. (1979) Ultrastructural observations in experimental hydrocephalus in the rabbit. *J. Neurol. Sci.* 43, 333-344.
42. Grinspan J.B., Stern J.L., Franceschini B. and Pleasure D. (1993) Trophic effects of basic fibroblast growth factor (bFGF) on differentiated oligodendroglia: a mechanism for regeneration of the oligodendroglial lineage. *J. Neurosci. Res.* 36, 672-680.
43. Harris N.G., McAllister J.P., Conaughty J.M. and Jones H.C. (1996) The effect of inherited hydrocephalus and shunt treatment on cortical pyramidal cell dendrites in the infant H-Tx rat. *Exp. Neurol.* 141, 269-279.
44. Harris N.G., Plant H.D., Briggs R.W. and Jones H.C. (1996) Metabolite changes in the cerebral cortex of treated and untreated infant hydrocephalic rats studied using in vitro ³¹P-NMR spectroscopy. *J. Neurochem.* 67, 2030-2038.
45. Heidemann S.R. and Buxbaum R.E. (1994) Mechanical tension as a regulator of axonal development. *Neurotoxicology* 15, 95-108.
46. Hildebrand C., Remahl S., Persson H. and Bjartmar C. (1992) Myelinated nerve fibers in the CNS. *Prog. Neurobiol.* 40, 319-384.
47. Hirayama A. (1980) Histopathological study of congenital and acquired experimental hydrocephalus. *Brain. Dev.* 2, 171-189.
48. Hochwald G.M. (1985) Animal models of hydrocephalus: recent developments. *Proc. Soc. Exp. Biol. Med.* 178, 1-11.
49. Hochwald G.M., Sahar A., Sadik A.R. and Ransohoff J. (1969) Cerebrospinal fluid production and histological observations in animals with experimental obstructive hydrocephalus. *Exp. Neurol.* 25, 190-199.
50. Jacobson S. (1970) Distribution of commissural axon terminals in the rat neocortex. *Exp. Neurol.* 28, 193-205.
51. James A.E., Flor W.J., Bush M., Merz T. and Rish B.L. (1974) An experimental model for chronic communicating hydrocephalus. *J. Neurosurg.* 41, 32-37.
52. James A.E., Flor W.J., Novak G.R., Strecker E.P., Burns B. and Epstein M. (1977) Experimental hydrocephalus. *Exp. Eye Res. Suppl.*, 435-459.
53. Jordan C., Friedrich V., Jr. and Dubois-Dalcq M. (1989) In situ hybridization analysis of myelin gene transcripts in developing mouse spinal cord. *J. Neurosci.* 9, 248-257.

54. Kapfhammer J.P. and Schwab M.E. (1994) Inverse patterns of myelination and GAP-43 expression in the adult CNS: neurite growth inhibitors as regulators of neuronal plasticity? *J. Comp. Neurol.* **340**, 194-206.
55. Karns L.R., Ng S.C., Freeman J.A. and Fishman M.C. (1987) Cloning of Complementary DNA for GAP-43, a neuronal growth-related protein. *Science* **236**, 597-600.
56. Kolodny E.H. (1993) Dysmyelinating and demyelinating conditions in infancy. *Curr. Opin. Neurosurg.* **6**, 379-386.
57. Kriebel R.M., Shah A.B. and McAllister J.P. (1993) The microstructure of cortical neuropil before and after decompression in experimental infantile hydrocephalus. *Exp. Neurol.* **119**, 89-98.
58. Krigman M.R. and Hogan E.L. (1976) Undernutrition in the developing rat: effect upon myelination. *Brain Res.* **107**, 239-255.
59. Kronquist K.E., Crandall B.E., Macklin W.B. and Campagnoni A.T. (1987) Expression of myelin proteins in the developing human spinal cord: cloning and sequencing of human proteolipid protein cDNA. *J. Neurosci. Res.*
60. LeVine S.M., Wong D. and Macklin W.B. (1990) Developmental expression of proteolipid protein and DM20 mRNAs and proteins in the rat brain. *Dev. Neurosci.* **12**, 235-250.
61. Leviton A. and Gilles F. (1996) Ventriculomegaly, delayed myelination, white matter hypoplasia, and "periventricular" leukomalacia: how are they related? *Pediatr. Neuro.* **15**, 127-136.
62. Lowry O.H., Rosenbrought N.J., Farr A.L. and Randall R.S. (1951) Protein measurement with the Folin phenol reagent. *J. Biol. Chem.* **193**, 265-275.
63. Ludwin S.K. (1997) The pathobiology of the oligodendrocyte. *J. Neuropathol. Exp. Neurol.* **56**, 111-124.
64. Ludwin S.K. (1988) Remyelination in the central nervous system and the peripheral nervous system. *Adv. Neurol.* **47**, 215-254.
65. Ludwin S.K. and Maitland M. (1984) Long-term remyelination fails to reconstitute normal thickness of central myelin sheaths. *J. Neurol. Sci.* **64**, 193-198.
66. Macklin W.B., Gardinier M.V., Obeso Z.O., King K.D. and Wight P.A. (1991) Mutations in the myelin proteolipid protein gene alter oligodendrocyte gene expression in jimpy and jimpy^{msd} mice. *J. Neurochem.* **56**, 163-171.
67. McAllister J.P., Morano R.A., R.A. I., Scroff D.V., Hale P.M. and Kriebel R.M. (1992) Synaptic plasticity following early and late decompression for infantile hydrocephalus. *Soc. Neurosci.* **18**, 1316 [Abstr].
68. McComb J.G. (1983) Recent research into the nature of cerebrospinal fluid formation and absorption. *J. Neurosurg.* **59**, 369-383.
69. McKay R. (1997) Stem cells in the central nervous system. *Science* **276**, 66-71.
70. Meiri K.F. and Gordon-Weeks P.R. (1990) GAP-43 in growth cones is associated with areas of membrane that are tightly bound to substrate and is a component of a membrane skeleton subcellular fraction. *J. Neurosci.* **10**, 256-266.
71. Milhorat T.H., Clark R.G., Hammock M.K. and McGrath P.P. (1970) Structural, ultrastructural, and permeability changes in the ependyma and surrounding brain favoring equilibration in progressive hydrocephalus. *Arch. Neurol.* **22**, 397-407.

72. Miller D.J. and Rodriguez M. (1995) Spontaneous and induced remyelination in multiple sclerosis and the Theiler's virus model of central nervous system demyelination. *Microsc. Res. Tech.* 32, 230-245.
73. Miller R.H. (1996) Oligodendrocyte origins. *Trends Neurosci.* 19, 92-96.
74. Milner R.J., Lai C., Nave K.A., Lenoir D., Ogata J. and Sutcliffe J.G. (1985) Nucleotide sequences of two mRNAs for rat brain myelin proteolipid protein. *Cell* 42, 931-939.
75. Miyagami M., Nakamura S., Murakami T., Koga N. and Moriyasu M. (1976) Electron microscopic study of ventricular wall and choroid plexus in experimentally-induced hydrocephalic dogs. *Neurol. Med. Chir. (Tokyo)* 16, 15-21.
76. Miyazawa T., Nishiye H., Sato K., Kobayashi R., Hattori S., Shirai T. and Obata K. (1992) Cortical synaptogenesis in congenitally hydrocephalic HTX-rats using monoclonal anti-synaptic vesicle protein antibody. *Brain Dev.* 14, 75-79.
77. Miyazawa T. and Sato K. (1991) Learning disability and impairment of synaptogenesis in HTX-rats with arrested shunt-dependent hydrocephalus. *Child's Nerv. Syst.* 7, 121-128.
78. Mori K. (1995) Current concept of hydrocephalus: evolution of new classifications. *Child. Nerv. Syst.* 11, 523-531.
79. Morrow D.R., Campbell G., Liebermann A.R. and Anderson P.N. (1993) Differential regenerative growth of CNS axons into tibial and peroneal nerve grafts in the thalamus of adult rats. *Exp. Neurol.* 120, 60-69.
80. Moss D.J., Fernyhogh P., Chapman K., Baizer L., Bray D. and Allsopp T. (1990) Chicken growth-associated protein GAP-43 is tightly bound to the actin-rich neuronal membrane skeleton. *J. Neurochem.* 54, 729-736.
81. Nacimiento W., Sappok T., Brook G.A., Toth L., Oestreicher A.B., Gispen W.H., Noth J. and Kreutzberg G.W. (1995) B-50 (GAP-43) in the rat spinal cord caudal to hemisection: lack of intraspinal sprouting by dorsal root axons. *Neurosci. Lett.* 194, 13-16.
82. Ng S.C. (1988) Cloning of human GAP-43: growth association and ischemic resurgence. *Neuron* 1, 133-139.
83. Nishizawa K. (1994) NGF-induced stabilization of GAP-43 mRNA is mediated by both 3'untranslated region and a segment encoding the carboxy-terminus peptide. *Biochem. Biophys. Res. Commun.* 200, 789-796.
84. Norton W.T. (1996) Do oligodendrocytes divide? *Neurochem. Res.* 21, 495-503.
85. Nyberg-Hansen R., Torvik A. and Bhatia R. (1975) On the pathology of experimental hydrocephalus. *Brain Res.* 95, 343-350.
86. Ogata J., Hochwald G.M., Cravioto H. and Ransohoff J. (1972) Light and electron microscopic studies of experimental hydrocephalus. Ependymal and subependymal areas. *Acta Neuropathol.* 21, 213-223.
87. Perrone-Bizzozero N.I., Cansino V.V. and Kohn D.T. (1993) Posttranscriptional regulation of GAP-43 gene expression in PC 12 cells through protein kinase C-dependent stabilization of the mRNA. *J. Cell Biol.* 120, 1263-1270.
88. Povlishock J.T. (1992) Traumatically induced axonal injury: pathogenesis and pathobiological implications. *Brain Pathol.* 2, 1-12.
89. Richards H.K., Pickard J.D. and Punt J. (1985) Local cerebral glucose utilization in experimental chronic hydrocephalus in the rat. *Z. Kinderchir.* 40 Suppl 1, 9.

90. Roach A., Boylan K., Horvath S., Prusiner S.B. and Hood L.E. (1983) Characterization of cloned cDNA representing rat myelin basic protein: absence of expression in brain of shiverer mutant mice. *Cell* **34**, 799-806.
91. Rosenthal A., Chan S.Y., Henzel W., Haskell C., Kuang W.J., Wilcox J.N., Ullrich A., Goeddel D.V. and Routtenberg A. (1987) Primary structure and mRNA localization of protein F1, a growth-related protein kinase C substrate associated with synaptic plasticity. *EMBO J.* **6**, 3641-3646.
92. Rubin R.C., Hochwald G., Tiell M., Liwnicz B. and Epstein F. (1975) Reconstitution of the cerebral cortical mantle in shunt-corrected hydrocephalus. *Dev. Med. Child Neurol. Suppl.* **35**, 151-156.
93. Russell D.S. (1949) Observations on the pathology of hydrocephalus. *Med. Res. Council Special Report Ser.* **265**, 1-138.
94. Schreyer D.J. and Skene J.H.P. (1991) Fate of GAP-43 in ascending spinal axons of DRG neurons after peripheral nerve injury: delayed accumulation and correlation with regenerative potential. *J. Neurosci.* **11**, 3738-3751.
95. Schreyer D.J. and Skene J.H.P. (1993) Injury-associated induction of GAP-43 expression displays axon branch specificity in rat dorsal root ganglion neurons. *J. Neurobiol.* **24**, 959-970.
96. Shiota C., Ikenaka K. and Mikoshiba K. (1991) Developmental expression of myelin protein genes in dysmyelinating mutant mice: analysis by nuclear run-off transcription assay, in situ hybridization, and immunohistochemistry. *J. Neurochem.* **56**, 818-826.
97. Sorg B.J.A., Smith M.M. and Campagnoni A.T. (1987) Developmental expression of the myelin proteolipid protein and basic protein mRNAs in normal and dysmyelinating mutant mice. *J. Neurochem.* **49**, 1146-1154.
98. Strittmatter S.M., Vartanian T. and Fishman M.C. (1992) GAP-43 as a plasticity protein in neuronal form and repair. *J. Neurobiol.* **23**, 507-520.
99. Tagaya M., Matsuyama T., Nakamura H., Hata R., Shimizu S., Kiyama H., Matsumoto M. and Sugita M. (1995) Increased F1/GAP-43 mRNA accumulation in gerbil hippocampus after brain ischemia. *J. Cerebral Blood Flow Metabol.* **15**, 1132-1136.
100. Takei F., Shapiro K. and Kohn I. (1987) Influence of the rate of ventricular enlargement on the white matter water content in progressive feline hydrocephalus. *J. Neurosurg.* **66**, 577-583.
101. Takei F., Shapiro K., Oi S. and Sato O. (1994) The efficacy of shunting hydrocephalic edema. *Acta Neurochir. Suppl.* **60**, 577-581.
102. Tauber H., Waehneltd T.V. and Neuhoff V. (1980) Myelination in rabbit optic nerves is accelerated by artificial eye opening. *Neurosci. Lett.* **16**, 235-238.
103. Tetzlaff W., Alexander S.W., Miller F.D. and Bisby M.A. (1991) Response of facial and rubrospinal neurons to axotomy: changes in mRNA expression for cytoskeletal proteins and GAP-43. *J. Neurosci.* **11**, 2528-2544.
104. Timsit S., Martinez S., Allinquant B., Peyron F., Puelles L. and Zalc B. (1995) Oligodendrocytes originate in a restricted zone of the embryonic ventral neural tube defined by DM-20 mRNA expression. *J. Neurosci.* **15**, 1012-1024.
105. Timsit S.G., Bally-Cuif L., Colman D.R. and Zalc B. (1992) DM-20 mRNA is expressed during the embryonic development of the nervous system of the mouse. *J. Neurochem.* **58**, 1172-1175.

106. Torvik A. and Stenwig A.E. (1977) The pathology of experimental obstructive hydrocephalus. Electron microscopic observations. *Acta Neuropathol.* 38, 21-26.
107. Tuor U.I., Del Bigio M.R. and Chumas P.D. (1996) Brain damage due to cerebral hypoxia/ischemia in the neonate: pathology and pharmacological modification. *Cerebrovasc. Brain Metab. Rev.* 8, 159-193.
108. Vaudano E., Campbell G., Anderson P.N., Davies A.P., Woolhead C., Schreyer D.J. and Lieberman A.R. (1995) The effects of a lesion or a peripheral nerve graft on GAP-43 upregulation in the adult rat brain: an in situ hybridization and immunocytochemical study. *J. Neurosci.* 15, 3594-3611.
109. Verhaagen J., Zhang Y., Hamers F.P.T. and Gispen W.H. (1993) Elevated expression of B-50 (GAP-43)-mRNA in a subpopulation of olfactory bulb mitral cells following axotomy. *J. Neurosci. Res.* 35, 162-169.
110. Vitkovic L. (1992) GAP-43 expression in macroglial cells: potential functional significance. *Persp. Dev. Neurobiol.* 1, 39-43.
111. Weibel E.R. (1979) *Stereological Methods. Vol. 1 Practical Methods for Biological Morphometry.*, pp. 415pp. Academic Press, Inc., London.
112. Weller R.O., Mitchell J., Griffin R.L. and Gardner M.J. (1978) The effects of hydrocephalus upon the developing brain. Histological and quantitative studies of the ependyma and subependyma in hydrocephalic rats. *J. Neurol. Sci.* 36, 383-402.
113. Wiggins R.C. (1986) Myelination: a critical stage in development. *Neurotoxicology* 7, 103-120.
114. Yamada H., Yokota A., Furuta A. and Horie A. (1992) Reconstitution of shunted mantle in experimental hydrocephalus. *J. Neurosurg.* 76, 856-862.
115. Yamada K., Goto S., Oyama T., Inoue N., Nagahiro S. and Ushio Y. (1994) In vivo induction of the growth associated protein GAP-43/B-50 in rat astrocytes following transient middle cerebral artery occlusion. *Acta Neuropathol.* 88, 553-557.
116. Yanker B.A., Benowitz L.I., Villa-Komaroff L. and Neve R.L. (1990) Transfection of PC-12 cells with the human GAP-43 gene: effects on neurite outgrowth and regeneration. *Mol. Brain Res.* 7, 39-44.